journal

J. Am. Ceram. Soc., ■■ [■■] 1–5 (2010)
DOI: 10.1111/j.1551-2916.2010.03697.x

Monolithic Glass Scaffolds with Dual Porosity Prepared by Polymer-Induced Phase Separation and Sol–Gel

Yuliya Vueva,[†,‡] Ana Gama,[‡] Alexandra V. Teixeira,[‡] Rui M. Almeida,[‡] Shaojie Wang,[§] Matthias M. Falk,[¶] and Himanshu Jain[§]

[‡]Departamento de Engenharia de Materiais/ICEMS, Instituto Superior Tecnico/TULisbon 1049-001 Lisbon, Portugal

[§]Department of Materials Science and Engineering, Lehigh University, Bethlehem, Pennsylvania 18015

[¶]Department of Biological Sciences, Lehigh University, Bethlehem, Pennsylvania 18015

Sol–gel-derived SiO_2–CaO–P_2O_5 porous glass monoliths with a dual hierarchical pore structure including both macropores of ~20–200 micrometers and mesopores ~5–20 nanometers in size are prepared in the presence of the drying control chemical additive formamide, for a possible application as scaffolds in bone tissue regeneration. While the mesopores are intrinsic to the sol–gel processing, the interconnected macropores are achieved through a polymer-induced phase separation together with the sol–gel transition, by adding a water-soluble polymer, poly(ethylene oxide), to the precursor sol. The textural nanopore structure is controlled through solvent exchange procedures and the addition of urea. The overall pore size distribution obtained by mercury intrusion porosimetry was found to shift to larger pore sizes when formamide is added. *In vitro* tests are used to evaluate the bioactivity. The cell-support function of the resultant scaffolds is also assessed *in vitro* using osteoblast-like cells cultured for 2 days. The results show that the scaffold has a significant bioactivity and a good ability to support the attachment of MC3T3 preosteoblast cells.

I. Introduction

Tissue engineering is a technology based on the principle that the living body has the potential for regeneration; it combines engineering and cell biology concepts towards the creation (growth) of new human tissue.[1] One significant branch of tissue engineering involves the use of engineered materials with high porosity, termed as scaffolds, designed to act as (temporary) three dimensional templates for cell adhesion, proliferation, migration, and ultimately the formation of new tissue.[2] An important class of scaffolds for bone tissue engineering is based on bioactive and biodegradable ceramics and glasses. An alternative approach to conventional melt quenching for the fabrication of bioactive glass is the sol–gel technique, a low-temperature chemical route to the fabrication of glass through the hydrolysis and condensation of metal alkoxide precursors to form a sol and the gelation of the sol to obtain a gel, which is heat treated to form a glass.[3] The sol–gel process enables the control of the main factors that affect bioactivity, namely composition (e.g., Ca/Si molar ratio) and texture (pore size and shape). Moreover, sol–gel-derived bioactive glasses tend to be more bioactive and resorb quicker than melt-derived glasses of similar compositions because of the intrinsic nanometer-scale porosity of the former.[4]

In order to create a macroporous network, a few possible methods exist. For instance, Sepulveda *et al.*[5] and, more recently, Jones *et al.*[6] have reported the preparation of macroporous (>100 μm) matrices by foaming sol–gel systems, where a surfactant (e.g., Teepol) was added to a sol prepared from a mixture of alkoxides. A second possible technique to create macroporosity in materials is Maekawa *et al.*'s method,[7] where macroporous templates such as a polystyrene foam or an oil-in-water emulsion are used. Another method is based on polymer-induced phase separation,[8,9] where organic polymers such as poly(ethylene oxide) (PEO), poly(ethylene glycol) (PEG), or poly(acrylic acid) (PAA) are added to an alkoxide mixture, causing phase separation by spinodal decomposition parallel to the sol–gel transition; a subsequent heat treatment causes the burnout of the organic polymer phase, leading to a coral-like morphology with interconnected macropores.[10]

The most critical stage for producing sol–gel glass monoliths is the drying process. During the initial stage of drying, evaporation of the liquid from the micropores in the gel causes the development of large capillary stresses, which can initiate cracking. In order to overcome this problem, a number of methods have been developed like "slow rate evaporation,"[11] supercritical drying,[12] or the use of a drying control chemical additive (DCCA) such as formamide,[13] dimethylformamide,[14] or acetonitrile.[15] Addition of a DCCA allows drying at elevated temperatures and ambient pressure without crack formation, leading to a change in the structure of the sol–gel-derived material. Firstly, the DCCA causes the generation of large pores with a narrow size distribution.[16] Because of the larger pore size, capillary forces will be weaker and hence the stresses exerted on the pore walls during drying will be smaller; furthermore, as the vapor pressure is higher within larger pores, according to the Kelvin equation, the increased pore size promotes the evaporation of the solvents.[17] The second mechanism is due to the binding of the DCCA to the silica surface through the formation of hydrogen bonds; this will facilitate the removal of water molecules by preventing their interaction with the silanol groups on the pore walls.

In this work, sol–gel glasses with dual hierarchical porosity at both the nano (~5–20 nm) and the macroscale (~20–200 μm) have been prepared on the basis of polymer-induced phase separation using PEO. In order to improve the mechanical strength of the scaffolds and to reduce crack formation and shrinkage of the gels, formamide was used as a DCCA.

II. Experimental Procedure

Glass scaffolds with the nominal composition 60 SiO_2–36 CaO–4 P_2O_5 (in mol%) were synthesized using sol–gel and a polymer-induced phase separation technique. The starting sols were prepared by dissolving 1.4 g PEO, with an average molecular weight of 100 000, in 0.05 N acetic acid (CH_3COOH) aqueous

S. Bose—contributing editor

Manuscript No. 26995. Received October 22, 2009; approved January 26, 2010.
This work was financially supported by NSF's International Materials Institute for New Functionality in Glass (Grant Nos. DMR-0409588 and DMR-0844014) and the Fundação para a Ciência e a Tecnologia, through PORSCAF project (No. PTDC/CTM/66712/2006).
[†]Author to whom correspondence should be addressed. e-mail: yuliya.vueva@ist.utl.pt

solution. To this solution, tetramethoxysilane (TMOS, TMOS:0.05 N aqueous CH_3COOH molar ratio $\sim$0.06) plus formamide (CH_3NO) (formamide:TMOS ratio = 0.8) and, in selected cases, urea also (CH_4N_2O) (urea:TMOS ratio = 0.25), were added under vigorous stirring (total volume of the reaction mixture $\sim$45 mL). Calcium nitrate tetrahydrate ($Ca(NO_3)_2 \cdot 4H_2O$) and triethyl orthophosphate (TEP) were then added and stirred until dissolution of the calcium salt. To accelerate gelation, aqueous hydrofluoric acid (HF, 2.5 wt %) was also added and the solution was kept at 40°C until gelation occurred. Solvent exchange was performed on selected samples by immersing well-aged gels, while still wet, in deionized water at room temperature, for 3 h, and then in 1N ammonia (NH_4OH) aqueous solution for 4 days, at 40°C. The resulting gel was dried in an atmosphere with controlled relative humidity (RH = 90%) at 60°C for 1 day and at 180°C for 2 days; then, they were heat treated sequentially at 600°C (1 h) and 700°C (2 h), with heating and cooling (to room temperature) rates of 100°C/h.

The pore morphology and textural features of the heat-treated gel samples (coated with iridium) were observed by field-emission scanning electron microscopy (FE-SEM, Hitachi 4300, Pleasanton, CA), at 5 kV. The interconnected pore size distribution, as well as the volume fraction of porosity and density, were measured using mercury intrusion porosimetry (Autopore IV, Micromeritics Co., Norcross, GA).

The *in vitro* bioactivity of the scaffolds was assessed by soaking them in a simulated body fluid solution (SBF,[18] 0.01 g/mL), at pH = 7.4 and 37°C, for a period of 10 days. The samples were removed from the SBF and washed with acetone to terminate the reaction; they were then dried and characterized by X-ray diffraction (XRD) and FE-SEM. A Philips diffractometer (Philips X'Pert APD, Philips, Almelo, the Netherlands) was used for XRD measurement of the samples in the powder form, using Cu$K\alpha$ radiation in the 2θ range of 5°–80°.

Diffuse reflectance infrared Fourier transform spectra (DRIFTS) were also collected (Nicolet 5700 spectrometer, Madison, WI) by removing and grinding the surface layer of the scaffolds and mixing it with KBr (the KBr:sample mass ratio was 1:10) to avoid specular reflection).

The cell response of the fabricated porous scaffolds was evaluated, after 2 days of MC3T3 preosteoblast cell culture, using 89% Alpha Minimum Essential Medium supplemented with 10% fetal bovine serum and 1% penn/strep (antibiotic). The cells were kept in an incubator, where a temperature of 37°C, 5% CO_2 atmosphere, and 100% RH conditions were maintained. The osteoblasts were harvested by trypsinization and seeded on glass scaffold samples (at 30 000 cells/cm^2). The cells were fixed, dehydrated (by graded ethanol), and observed under FE-SEM, 48 h after seeding.

III. Results and Discussion

In the preparation of glass scaffolds by the sol–gel method, a very critical stage is the drying step, when cracking and shrinkage occur. It is difficult to obtain crack-free sol–gel monoliths by direct drying of wet gels. To overcome this problem and to obtain scaffolds with sufficient mechanical stability, formamide was used as DCCA, whose low surface tension facilitates solvent evaporation.[17] The drying process was performed in a controlled high humidity atmosphere (90% RH), which also attenuated cracking during drying. As a result, large cracks were successfully eliminated, as shown in Fig. 1, for monolithic samples with a diameter of 13 mm and a thickness of 5 mm.

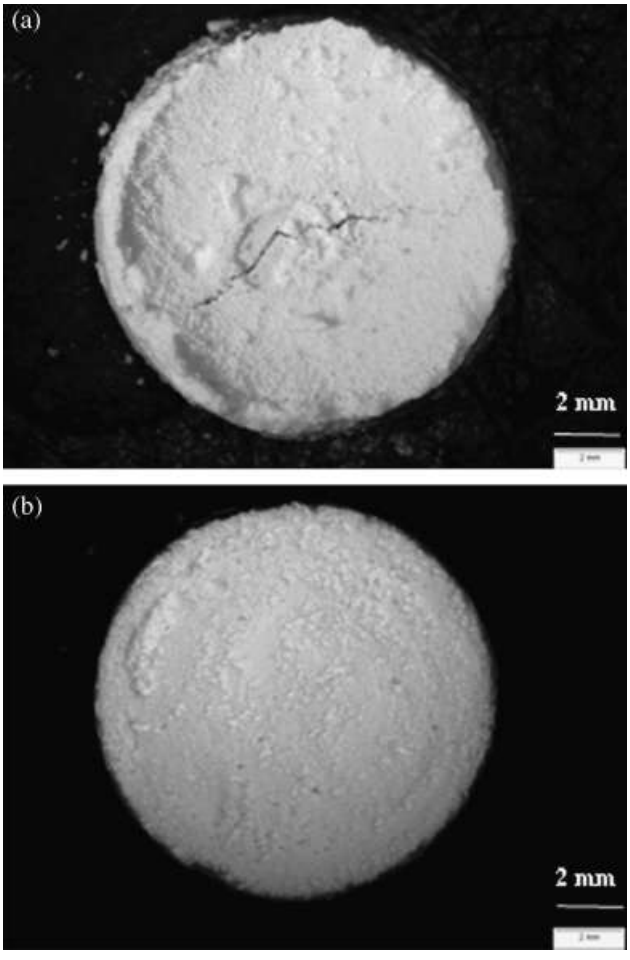

Fig. 1. Photographs of glass scaffolds: (a) a cracked sample prepared without formamide; (b) a crack-free sample prepared with formamide.

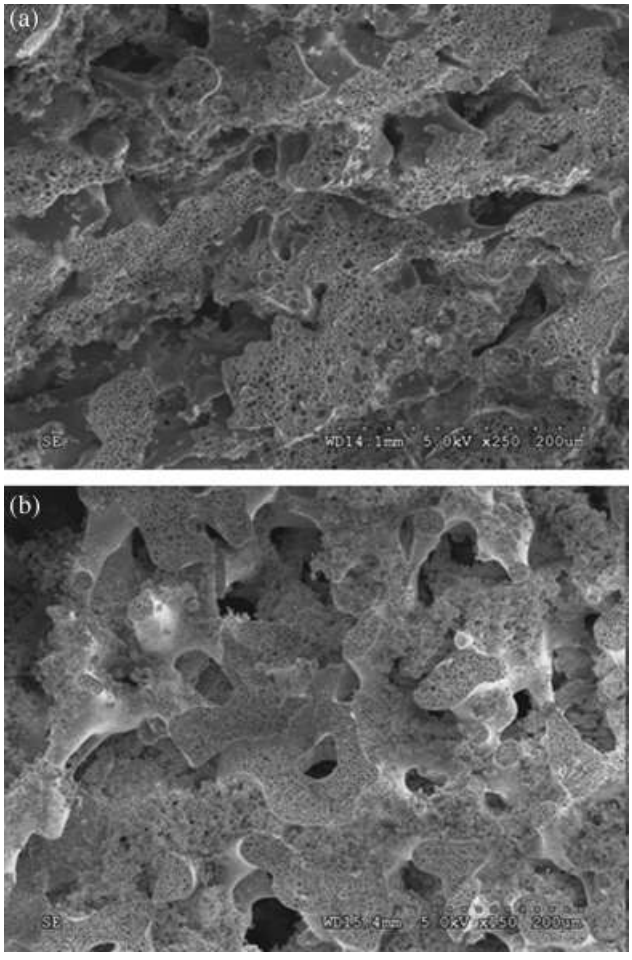

Fig. 2. Field-emission scanning electron microscopic micrographs of glass scaffolds of nominal composition 60 SiO_2–36 CaO–4 P_2O_5 (mol%): (a) prepared without formamide; (b) prepared with formamide.

The morphologies of glass scaffolds prepared without and with formamide are shown in Figs. 2(a) and (b), respectively. The interconnected macroporous network within a coral-like skeleton is clearly visible in both samples, which is desirable for scaffold function. The use of formamide appears to promote larger macropore sizes up to ~200 μm. Within the macrochannels, numerous micrometer-sized particle aggregates are also visible, which may have resulted from a secondary phase-separation phenomenon.[19]

The interconnected pore size distributions were obtained from mercury intrusion porosimetry. They are shown for scaffolds prepared without and with formamide in Fig. 3. While the former sample exhibited a bimodal distribution with a macropore size peak at 45 μm and a mesopore peak at 14 nm, in the sample prepared with formamide, the macropore peak shifted to ~84 μm (ranging from ~4 to 200 μm) and the mesopore peak also shifted upward to ~20 nm. The volume fraction of porosity of the heat-treated samples was 71% in the former case and 76% in the latter.[20]

The addition of formamide to the sols influences the hydrolysis and condensation reactions, modifies the sol–gel transition, and changes the gel morphology.[21] The action of formamide on the hydrolysis rate has been explained on the basis of hydrogen bonding and solvent viscosity.[22] Because of its high dielectric constant and dipole moment, formamide, which is able to form hydrogen bonds through its N and O atoms, may bond strongly to protons or hydroxyl groups, reducing the effective catalyst activity and hence the hydrolysis rate. An increased viscosity of the sol due to the addition of formamide may also affect the mobility of the chemical species in solution and hinder the hydrolysis mechanism.[23] In the gels prepared with formamide, the condensation reactions proceed faster due to an increase in pH, and the gelation[24] and phase separation are initiated earlier. As a result, gels with a higher macropore volume fraction are obtained. Urea also increases the pH and it is believed to act as a nanopore expander by generating aqueous ammonia *in situ*, having an effect, which adds to that of solvent exchange.[25]

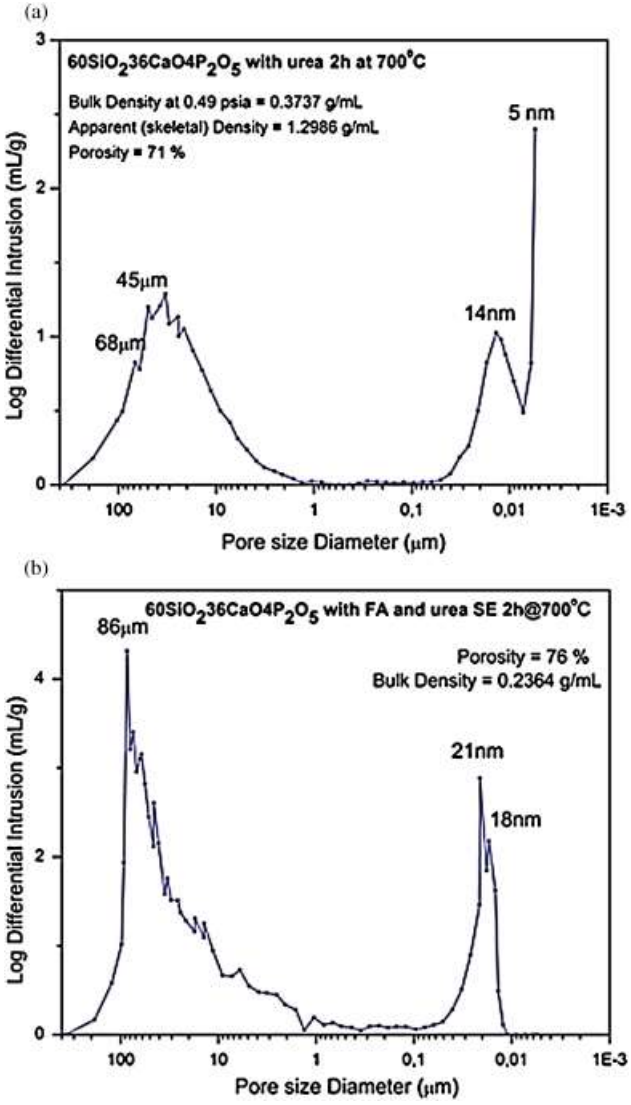

Fig. 3. Pore size distributions of 60 SiO_2–36 CaO–4 P_2O_5 scaffolds determined by mercury intrusion porosimetry: (a) a sample prepared without formamide; (b) a sample prepared with formamide.

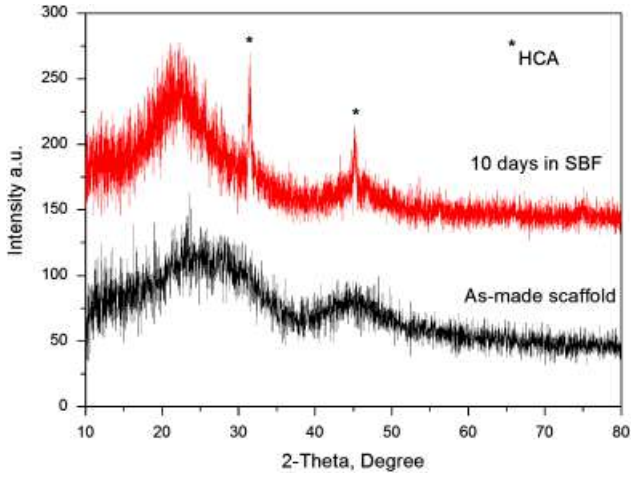

Fig. 4. X-ray diffraction patterns of bioactive glass scaffolds before (as-prepared) and after soaking in simulated body fluid solution. *HCA corresponds to hydroxycarbonate apatite.

The XRD patterns of an as-prepared glass scaffold and the glass scaffold after immersion for 10 days in SBF solution are shown in Fig. 4. The patterns of the as-prepared scaffold show broad peaks typical of an amorphous material. In comparison, the patterns of the scaffold immersed for 10 days in SBF solution contained peaks at 32° and 46° (2θ), corresponding to the (211) and (222) reflections of hydroxycarbonate apatite (HCA). This is a nonstoichiometric, carbonated form of hydroxyapatite (HA), which has a Ca/P ratio <1.67 (pure HA has the chemical formula $Ca_{10}(PO_4)_6(OH)_2$, with Ca/P = 1.67). The formation of HCA upon immersion in SBF is generally taken as a strong indication of the material bioactivity.[18]

In Fig. 5, for a 60 SiO_2–36 CaO–4 P_2O_5 scaffold, changes in the surface composition after soaking in SBF for 7 days are also

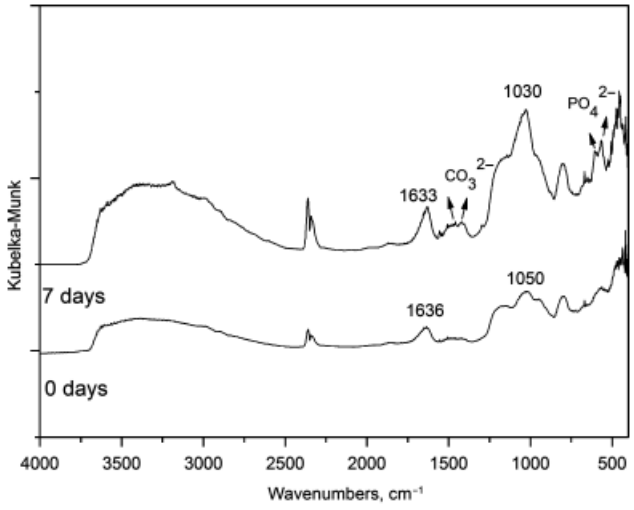

Fig. 5. Diffuse reflectance infrared Fourier transform spectra of 60 SiO_2–36 CaO–4 P_2O_5 porous glass sample before and after soaking in simulated body fluid solution for 7 days.

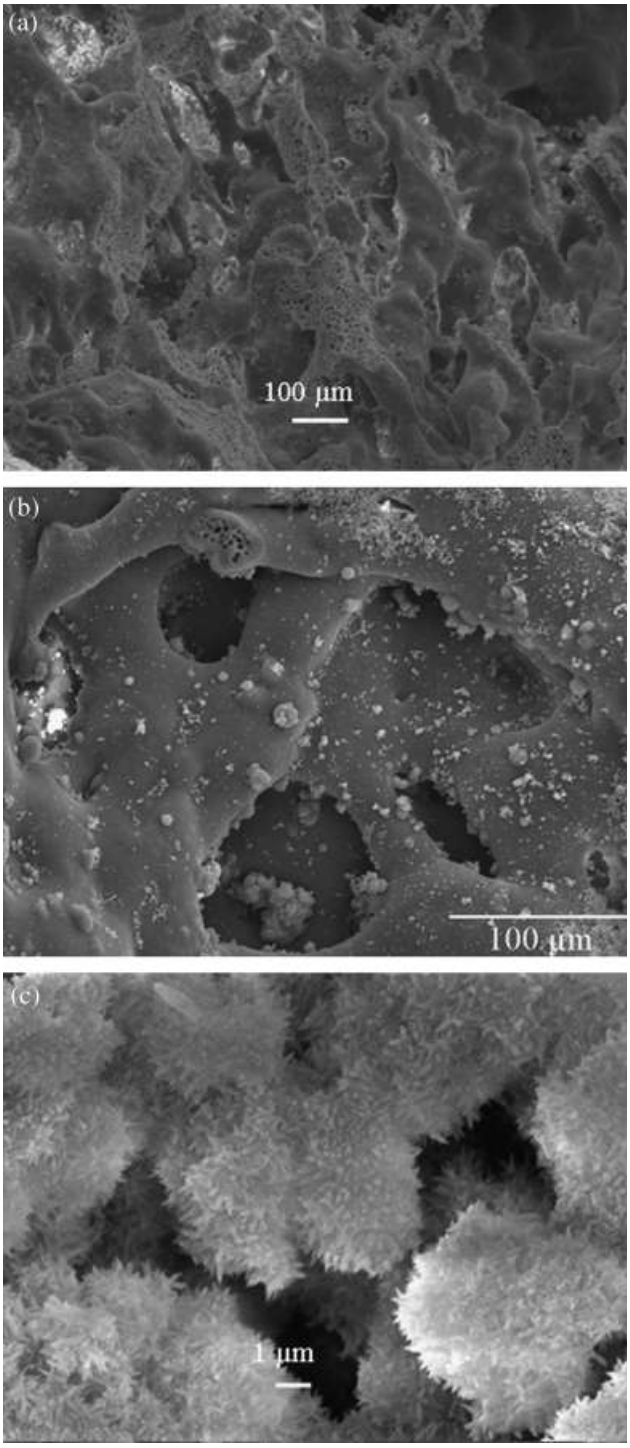

Fig. 6. Field-emission scanning electron microscopic micrographs of a bioactive glass scaffold: (a) before soaking in simulated body fluid solution (SBF); (b) after 10 days in SBF (scale bar 100 μm); (c) after 10 days in SBF (scale bar 1 μm).

indicated in DRIFTS spectra. The diffuse reflectance values were transformed into Kubelka–Munk units (k/S), expressing the ratio between the absorption (k) and scattering (S) coefficients of the samples at any given wavelength. The spectrum before soaking in SBF solution (0 days) exhibits typical silicate absorption bands at ca. 1050, 805, and 560 cm^{-1}. After soaking in SBF for 7 days, new bands appear at ca. 1030, 604 and 564 cm^{-1}, typical of P–O–P bending vibrations of PO_4^{3-} tetrahedra in crystalline calcium phosphate and characteristic carbonate absorption bands also appear at ca. 1484, 1420, and 874 cm^{-1}, indicating the formation of a carbonated HA layer upon immersion in SBF.[26]

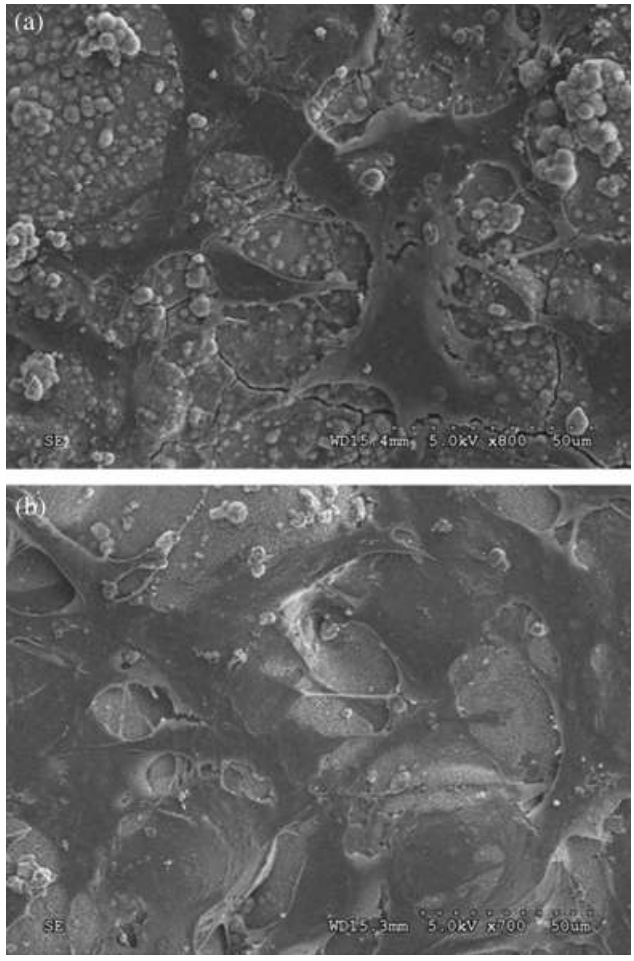

Fig. 7. Field-emission scanning electron microscopic micrographs of MC3T3 preosteoblast cells cultured for 2 days on a 60 SiO_2–36 CaO–4 P_2O_5 scaffold: (a) a sample prepared without formamide; (b) a sample prepared with formamide.

Figure 6 shows SEM images of a glass scaffold before and after immersion in SBF. Compared with the smooth walls of the macropores in the as-prepared scaffold (Fig. 5(a)), the surface of the scaffold after immersion for 10 days in SBF (Figs. 5(b) and (c)) was covered by needle-like crystals, presumably of HCA, based on the XRD results.

Figure 7 shows SEM micrographs of the morphologies of osteoblast cells 48 h after seeding on scaffolds. The osteoblast cells have a flattened, elongated, polygonal configuration and attach to the substrate through thin extensions, or filopodia. A comparison of Figs. 7(a) and (b) revealed that the cells have attached and proliferated more efficiently on scaffolds prepared with formamide. In fact, the SEM micrograph of Fig. 7(b) shows cells strongly adherent on the scaffold surface, with many protruding filopodia. A semiquantitative cell-attachment analysis was performed by calculating the percentage area of the SEM micrographs covered by cells, using the "Image J" software. The % area covered by cells on the sample prepared without formamide was 44% (Fig. 7(a)), whereas it was 73% for the sample prepared with formamide (Fig. 7(b)). These results suggest that the larger pores (both macro and mesopores) obtained through the use of formamide appear to ensure better cell adhesion, which is very important for a clinical application of the scaffolds.[27]

IV. Conclusions

Porous monolithic scaffolds of nominal molar composition 60 SiO_2–36 CaO–4 P_2O_5, with a dual pore structure including mesopores with sizes within the ~5–20 nm range and macropores with sizes up to ~200 μm, were prepared by the sol–gel method,

using polymer-induced phase separation as a precursor for interconnected macroporosity. Macroscopic cracking of the monoliths was successfully overcome by using formamide as DCCA. The average macropore as well as the mesopore size of the scaffolds were found to increase in the presence of formamide. These glassy materials showed good *in vitro* bioactivity, with XRD, DRIFTS, and SEM analysis confirming that, after 10 days in SBF, the surface of the scaffolds becomes covered by small crystals of HCA. SEM observations of cell cultures showed that the scaffolds had a good ability to support the attachment and spreading of osteoblast cells. The resultant scaffolds showed to be promising materials for bone tissue regeneration.

References

[1]J. P. Vacanti and C. A. Vacanti, *Principle of Tissue Engineering*, 2nd edition, Edited by R. P. Lanza, R. Langer, and J. P. Vancanti. Academic Press, San Diego, CA, 2000.

[2]Y. Ikada, "Challenges in Tissue Engineering," *J. R. Soc. Interface*, **3**, 589–601 (2006).

[3]C. J. Brinker and G. W. Scherrer, *Sol–Gel Science—the Physics and Chemistry of Sol–Gel Processing*. Academic Press, London, 1990.

[4]P. Sepulveda, J. R. Jones, and L.L Hench, "In Vitro Dissolution of Melt-Derived 45S5 and Sol–Gel Derived 58S Bioactive Glasses," *J. Biomed. Mater. Res*., **61** [2] 301–11 (2002).

[5]P. Sepulveda, J. R. Jones, and L. L. Hench, "Bioactive Sol–Gel Foams for Tissue Repair," *J. Biom. Mater. Res*., **59**, 340–8 (2002).

[6]J. R. Jones, L. M. Ehrenfried, and L. L. Hench, "Optimising Bioactive Glass Scaffolds for Bone Tissue Engineering," *Biomaterials*, **27**, 964–73 (2006).

[7]H. Maekawa, J. Esquena, S. Bishop, C. Solans, and B. F. Chmelka, "Meso/Macroporous Inorganic Oxide Monoliths from Polymer Foams," *Adv. Mater*., **15**, 591–6 (2003).

[8]K. Nakanishi, "Pore Structure Control of Silica Gels Based on Phase Separation," *J. Porous Mater*., **4**, 67–112 (1997).

[9]R. Takahashi, S. Sato, T. Sodesawa, T. Goto, K. Matsutani, and N. Mikami, "Bending Strength of Silica Gel with Bimodal Pores: Effect of Variation in Mesopore Structure," *Mater. Res. Bull*., **40**, 1148–56 (2005).

[10]A.C Marques, H. Jain, and R. M. Almeida, "Sol–Gel Derived Nano/Macroporous Scaffolds," *Phys. Chem. Glasses: Eur. J. Glass Sci. Technol. B*, **48**, 65–8 (2007).

[11]B. S. Shukla and G. P. Johari, "Effect of Ethanol on the Density and Morphology of Monolithic SiO_2 Glass Prepared by the Sol–Gel Method," *J. Non-Cryst. Solids*, **102** [2–3] 263–8 (1988).

[12]J. Zarzyscki, M. Prassas, and J. Phallipou, "Synthesis of Glasses from Gels: The Problem of Monolithic Gels," *J. Mater. Sci*., **17**, 3371–9 (1982).

[13]G. Orcel and L. Hench, "Effect of Formamide Additive on the Chemistry of Silica Sol–Gels: Part I: NMR of Silica Hydrolysis," *J. Non-Cryst. Solids*, **79** [1–2] 177–94 (1986).

[14]T. Adachi and S. Sakka, "The Role of N,N-Dimethylformamide, a DCCA, in the Formation of Silica Gel Monoliths by Sol–Gel Method," *J. Non-Cryst. Solids*, **99**, 118–28 (1988).

[15]I. Artaki, T. W. Zerda, and J. Jonas, "Solvent Effects on the Condensation Stage of the Sol–Gel Process," *J. Non-Cryst. Solids*, **81**, 381–95 (1986).

[16]F. Kirkbir, H. Murata, D. Meyers, S. R. Chaudhuri, and A. Sarkar, "Drying and Sintering of Sol–Gel Derived Large SiO_2 Monoliths," *J. Sol–Gel Sci. Technol*., **6**, 203–17 (1996).

[17]John D. Wright and Nico A. J. M. Sommerdijk, *Sol–Gel Materials Chemistry and Applications*. CRC Press, Boca Raton, FL, 2000.

[18]T. Kokubo and H. Takadama, "How Useful is SBF in Predicting In Vivo Bone Bioactivity," *Biomaterials*, **27**, 2907–15 (2006).

[19]A. C. Marques, H. Jain, C. Kiely, K. Song, C. J. Kiely, and R. M. Almeida, "Nano-Macroporous Monolithic Scaffolds Prepared by the Sol–Gel Method," *J. Sol–Gel Sci. Technol*., **51**, 42–7 (2009).

[20]V. Karageorgiou and D. Kaplan, "Porosity of 3D Biomaterial Scaffolds and Osteogenesis," *Biomaterials*, **26**, 5474–91 (2005).

[21]L. Orcel., G. Hench, I. Artaki, J. Jones, and T. W. Zerda, "Effect of Formamide Additive on the Chemistry of Silica Sol–Gels II. Gel Structure," *J. Non-Cryst. Solids*, **105**, 223–31 (1988).

[22]C. J. Brinker and G. W. Scherer, *Sol–Gel Science: The Physics and Chemistry of Sol–Gel Processing*. Academic Press, Boston, 1990.

[23]N. Viart and J. L. Rehspringer, "Study of the Action of Formamide on the Evolution of a Sol by pH Measurements and Fourier Transformed Infra-Red Spectroscopy," *J. Non-Cryst. Solids*, **195**, 223–31 (1996).

[24]H. Kaji, K. Nakanishi, and N. Soga, "Formation of Porous Gel Morphology by Phase Separation in Gelling Alkoxy-Derived Silica. Affinity between Silica Polymers and Solvent," *J. Non-Cryst. Solids*, **181**, 16–26 (1995).

[25]K. Nakanishi and N. Tanaka, "Sol–Gel with Phase Separation. Hierarchically Porous Materials Optimized for High-Performance Liquid Chromatography Separations," *Acc. Chem. Res*., **40**, 863–73 (2007).

[26]M. Vallet-Regi, A. M. Romero, C. V. Ragel, and R. Z. LeGeros, "XRD, SEM-EDS, and FTIR Studies of *In Vitro* Growth of an Apatite-Like Layer on Sol–Gel Glasses," *J. Biomed. Mater. Res*., **44**, 416–21 (1999).

[27]Q. Z. Chen, A. Efthymiou, V. Salih, and A. R. Boccaccini, "Bioglass-Derived Glass–Ceramic Scaffolds: Study of Cell Proliferation and Scaffold Degradation In Vitro," *J. Biomed. Mater. Res*., **84A**, 1049–60 (2008). □